Impact of wind loads on the resistance capacity of the transmission tower subjected to ground surface deformations

Qianjin Shu[1], Zhaohui Huang[2], Guanglin Yuan[1,*], Weiqing Ma[3], Sheng Ye[1], Jing Zhou[4]

[1] State Key Laboratory for Geomechanics & Deep Underground Engineering, Jiangsu Key Laboratory of Environmental Impact & Structural Safety in Engineering, School of Mechanics & Civil Engineering, China University of Mining & Technology, Xuzhou, Jiangsu 221116, China.

[2] Department of Civil and Environmental Engineering, College of Engineering, Design and Physical Science, Brunel University, Uxbridge, Middlesex, UB8 3PH, U.K.

[3] Department of Information Technology, Shanxi Yangquan Electric Power Corporation, Yangquan 045000, China.

[4] School of Control and Computer Engineering, North China Electric Power University, Beijing 102206 , China.

Abstract: In this paper, two 1:2 scaled substructure models for a typical 110 kV transmission tower were designed and fabricated. The scaled tower substructure models were tested subjected to the stretching movements of horizontal ground surface under different wind load conditions. The wind speeds were assumed to be 15 m/s and 30 m/s, respectively in this study. The deformations of the tested tower models and the stresses and strains within the different members of the tower were fully measured. A large amount of the comprehensive test data was generated. Also a FE model using ANSYS was developed and validated by the test data. The research indicated that wind load has a significant unfavourable influence on the resistance of the transmission tower subjected to the ground surface deformation. Also the research showed that it is possible to use the FE model for the analysis and design of power transmission towers under ground surface movements.

Keywords: Power transmission tower; scaled tower model; wind load; ground movements; axial stress.

[1,*] Corresponding author.

E-mail address: ygl65@cumt.edu.cn (G. Yuan)

Highlights:

- Design 2 half-scaled substructure test models for a typical 110 kV single-circuit power transmission tower subjected to wind load conditions;
- Conduct two tests on the scaled tower substructure to investigate the behaviour of the transmission tower subjected to the horizontal ground movement under wind load conditions;
- Develop a FE model using ANSYS for modelling the 110 kV single-circuit power transmission tower and validate the FE model by the test data generated in this research.

Introduction

In recent years, with the increasing demands on electric power supply, it is very important to enhance the safety of power transmission line. Hence, considerable efforts have been made by different researchers to investigate the behaviour of power transmission towers under different loading and environmental conditions [1-6]. In some countries, such as China, many power transmission towers have to pass across coal mining areas. Therefore, the failure of the transmission towers are often happened due to the ground surface cracking, subsidence, non-uniform settlement, etc [7-10].

Another natural hazard to cause the failure of transmission tower is the strong wind load acting on the tower, resulted from tropical cyclones and tornados [11-13]. Hence, for the safety design of transmission towers in geological disaster areas, it is important to understand the behaviour of the transmission tower subjected to the combined effects of wind load and ground surface deformations.

Xie et al. [13] carried out an experimental study on a scaled tower model for a typical 500 kV transmission tower under strong wind load. The test investigated the failure mechanism of the transmission tower under combined static load and equivalent wind load. Momomura et al. [14] and Okamura et al. [15] investigated the dynamic characteristics of the transmission towers in mountainous areas. Yasui et al. [16] analysed the wind induced dynamic characteristics of the transmission towers with various bracing systems. A 1:2 scaled tower model was designed and tested by Moon et al. [12] to assess the failure mode of the transmission towers under wind load. Mara et al. [17, 18] studied the effect of wind direction on the response and resistance capacity of a transmission tower, and evaluated the tower capacity by considering the uncertainty in material properties and geometric variables. These researches have well revealed the failure mechanisms of the transmission towers under wind loads.

In recent years, a number of researches have been done to assess the safety of the transmission lines in mining areas. The Island Creek Coal Company in Virginia enabled coal mining under high-voltage transmission towers through the controlling of the subsiding and deformation of

ground surface by grouting [19]. Bruhn et al. [20] studied the response of the transmission towers subjected to ground deformations. White [21] reported an investigation of the effect of mining on transmission towers. Based on FE analysis for a typical transmission tower, Yuan et al. [22, 23] studied the structural behaviour of the transmission towers subjected to ground movements. They conducted an experimental test on a scaled tower model based on a typical 500 kV self-supporting transmission tower. Shu et al. [24] studied numerically the failure modes of the transmission towers in mining areas to obtain the limit state displacement of the supports under the ground surface deformations. Li et al. [25] investigated the effect of coupled interaction between vertical load and the ground surface deformation.

As mentioned above, according to the authors' knowledge, there were no experimental studies which have been conducted to study the structural behaviour of the transmission tower under combined wind load and ground deformation. Hence, the main objectives of this research are:

- Develop a FE model using ANSYS for modelling a typical prototype of 110 kV power transmission tower under combined wind loads and horizontal ground surface motion. Based on the FE analyses, two 1:2 scaled sub-structure tower model are designed and fabricated.
- Conduct the two tests on the 1:2 scaled sub-structure tower model with isolated tower leg's foundations to investigate the behaviour of the 110 kV power transmission tower under both the wind loads and horizontal ground surface motions. In this research the wind speeds acting on the towers were assumed to be 15 m/s and 30 m/s. The tests generate a series of valuable data on the failure modes of the transmission tower; stress and strain states within the structural members of the tower and the relationship between the tower's deformations and support's movements.
- Validate the developed FE model, using the test data, for modelling 110 kV power transmission tower with isolated tower leg's foundations under both wind loads and horizontal ground surface movements.

Experiment's design and implementation

2.1 Design of the scaled tower substructure models

The prototype of full tower selected here is a typical 110 kV single-circuit tower. As shown in Fig. 1, the total height of the tower is 26.7 m. The support spacing is 4.035 m in the direction normal to the power line, and 3.125 m along the power line. According to the references [22-24], it is reasonable to select the lower part of the tower (within the rectangular dash line, as shown in Fig. 1) as the prototype of the 1:2 scaled tower substructure model (called scaled tower model in the rest of this paper). As shown in Fig. 2, the height of the scaled tower model is 4 m, the dimensions of the top and bottom of the scaled tower model are 1530×1200 mm and 2018×1563 mm, respectively.

The scaled tower models were fabricated in the State Grid Jiangsu Huadian Steel Tower Manufacturing Co., Ltd. The tower's legs were made of hot-rolled angle steel, and the bracings, diaphragms and subsidiary members were made of cold worked angle steel. The sectional details of the structural members of the prototype tower substructure and scaled tower model are given in Table 1. The tested yield strengths of the steel angles are listed in Table 2. The bolts used in the prototype whole tower were the Grade 4.8 galvanized M16 bolts. According to the scale of 1:2, the bolts used for the scaled tower model should be not less than Grade 4.8 M8 bolts. In order to avoid the premature failure of the joints caused by the bolts' stress concentration, in this study the Grade 8.8 galvanized M8 bolts were used. To keep the bolt pre-tightening force as constant, the tightening torque was controlled in accordance with the standards of magnitude 4.8 M8 bolts. The yield torque of the Grade 8.8 galvanized M8 bolts was calculated based on the Chinese National Standard (GB/T 16823.2-1997), which was 18.1 N.m. Hence, in this research, the tightening torque of the bolts for the scaled tower model was set to be 18 N.m.

2.2 Load and support's displacement

Research conducted by Manis and Bloodworth [26] indicated that for the case of UK transmission towers it is the 45 degree wind orientation that gives lower load capacity of the tower due to one leg becomes more heavily loaded in compression rather than two. Previous design experience indicated that, for those towers without influence by mining subsidence, the 45 degree wind orientation normally gives failure of tower's leg while the 90 degree wind orientation gives failure of X-cross bracing members. The background of this research is to consider the behaviour of the transmission towers located in the subsidence areas caused by coal mining. Previous research [27] pointed out that one of the main failure modes of the transmission towers subjected to horizontal ground movement is the failure of X-cross bracing members. Therefore, in this research, only the ground

deformation and wind load along the direction perpendicular to the wire is considered. The test results will be used to validate finite element model. The validated FE model can be used to investigate in more details for the influences of different ground deformation and wind load directions on the behaviours of the towers.

In this research, the combined wind load, normal vertical load due to self-weight of the tower and power line and support's movement resulted from the ground movement were considered. The wind speed considered in this test was based on the current design recommendation specified in Chinese code for the prototype transmission tower. The maximum wind speed of the tower in the design is 30 m/s. In order to take into account the influence of different wind speeds, a wind speed of 15 m/s was also used for comparison. The comparison can clearly reveal the influence of wind load on the tower's ability to resist ground surface deformation caused by mining. Hence, for the wind load, two wind speeds of 15 m/s and 30m/s with the direction normal to the power line were used.

Table 3 lists the wind load and the vertical loads acting on the prototype of the whole tower. The loads applied to the scaled tower model were calculated based on the loads of the prototype of the whole tower using the similarity law of equal stress. In particular, the vertical loads acting on the top of the scaled tower model's four legs were 1/4 times of the loads acting on the same section of the prototype tower.

In this research for simplicity the eccentric vertical load due to the deformation of the upper part of the tower was ignored in the tests. Due to the limitation of the lab's conditions, the dynamic wind load was not considered as well. Based on the previous research [17, 18] the equivalent wind load, as shown in Fig. 3, was used in this study. The horizontal ground surface deformation was simulated by synchronously jacking two of the adjacent supports outwards normal to the power line. The direction of the wind load and the support's stretching are schematically shown in Fig. 3. The stretching displacements of supports were generated by the jacks as shown in Fig. 7.

2.3 Validation of the scaled tower model using finite element method

To make sure the scaled tower model can reasonably represent the behaviour of the whole tower under the wind load and horizontal ground movement, both the scaled tower model and whole tower were analysed using ANSYS, respectively. In this FE model the members of the tower's legs, cross bracings and horizontal diaphragms were modelled using BEAM188 elements, and the subsidiary members were modelled with LINK180 elements [22-24]. All of the joints between beam elements were assumed full moment connections while the joints between beam elements and link elements were all pinned connections. No slippage was considered for all connections. Both the

material and geometric nonlinearities were considered for the modelling. An ideal elastic-plastic model was used to simulate the mechanical behaviours of the angle steel material. The elastic modulus of the steel angles was 2.06×10^5 N/mm^2, the Poisson's ratio was 0.3. As shown in Table 2, the yield strengths of the different structural members were used for the FE analyses of both whole tower and scaled tower model.

Due to limit space, only the case, which the wind load acted on the tower at a speed of 30 m/s with the wind direction normal to the power line and the supports were stretched out in the same direction (i.e., supports A & D were fixed, supports B & C were jacked outward, see Fig. 3), is presented here. Apart from the wind load, the scaled tower model was also subjected to the self-weight of the upper structure, conductors, ground wire, insulators and accessories at the same time. These loads were calculated based on the actual load combination of the prototype tower (whole tower) using the similarity law of equal stress, as mentioned above.

The deformed shapes of the whole tower and scaled tower model are showed in Fig. 4. Fig. 5 shows the comparisons of the predicted axial forces of some key members for the whole tower and the scaled tower model. It is evident that the failure modes are similar, exhibiting out-of-plane bending of the first cross bracing member F11 (see Fig. 6 for member position). The changes of axial forces in some key members are close to each other, especially in the elastic stage. The difference of applied displacements corresponding to the peak axial forces in the member F11 is less than 5%. Also, the difference of the peak axial forces in F11 is within 10%. Therefore, the structural behaviours between the scaled tower model and whole tower structure are very similar. Hence, the scaled tower model can be confidently used to represent the whole tower structure in this research.

2.4 Loading and measurement

The loading scheme for the scaled tower model is shown in Fig. 7. The actual loads acting on the scaled tower model is represented in Fig. 7a, which are the equivalent loads transferred from the upper part of the structure. The loads include concentrated loads, G, acting on the four top corners of the scaled tower model, the total wind load, F_w, and the equivalent moment M_w acting on the top of the scaled tower model. The vertical load of G was calculated from the self-weight of the upper part of the tower (including the tower assemblage and accessories) and the wires. M_w and F_w were calculated according to the wind speed, windward area, wire wind load and height variation coefficient of the wind pressure. Fig. 7b shows the applied equivalent loads on the scaled tower model, in which the horizontal force F_1 was used to generate equivalent moment, M_w and the cantilever length of M_w was 2300 mm. As shown in Fig. 8a, the equivalent horizontal load F_2 was

applied by chain blocks with tension sensors. Based on the static equilibrium condition $F_1 = M_w/D$ and $F_2 = F_1 + F_w$. In the test, the load G was applied by weights hanging at the four top corners of the scaled model, G = 350 kg. F1 and F2 were respectively 7.53 kN and 10.11 kN for the wind speed of 15 m/s, and 24.78 kN and 33.27 kN at the wind speed of 30m/s.

The stretching displacement of the supports was generated by the jacks in the direction normal to the power line (see Fig. 3). Fig. 8 shows the loading system used in this research.

2.5 Measuring scheme

In these tests, the horizontal displacements of supports were measured by YHD-200 displacement meters produced by Cangzhou Xinyi Experimental Instruments Ltd., one at each support along the direction perpendicular to the power line. As shown in Fig. 8b, a total of four horizontal translational displacements of the supports were recorded. DH801-750 guyed displacement meters produced by Jiangsu Donghua Testing Technology Limited Company were used to measure the displacements on the top corners of the scaled tower model. As shown in Fig. 9, Meters no. 1 to 4 were used to measure the horizontal displacements and the Meters no. 5 to 8 were used to measure the vertical displacements.

Fig. 6 shows the arrangement of the strain gauges in the truss members of the scaled tower model. As shown in Fig. 6, there were three strain gauges fixed along the tower's leg B (at positions Z6 to Z15). All three strains gauges were orientated in the axial direction of the tower's leg (see Fig. 10a). For other truss members, only two strain gauges were allocated on the centre of angle flanges (see Fig. 10b).

The forces applied through actuators, chain blocks and jacks were measured using JLBT-5T load transducers.

2.6 Test procedure

The tests were performed in the State Key Laboratory for Geomechanics & Deep Underground Engineering in the China University of Mining & Technology. The testing procedure was as follows:

(1) Assembling the H-section steel beams platform, mounting the scaled tower model onto the platform, adjusting the elevation for the supports of the scaled tower model, mounting loading and measuring devices;

(2) Fixing temporarily the H section beam of the movable part of the platform, packing the steel loading blocks on the loading platform which applied the vertical loads on the four top

corners of the scaled tower model, applying the equivalent wind loads (either 15 m/s or 30 m/s) step by step until the total wind load was reached, keeping the total loads unchanged during the test;

(3) Unfixing the H section beam, using jacks to apply the horizontal stretching displacement loads on the two of the supports, with 1 mm loading step. During loading procedure, the forces in the chain blocks and actuators were kept constant. The displacement load was increased step by step until significant deformation occurred in the truss members or the reaction forces exhibited dropping. All the measured parameters were recorded step by step by the computer via the data collection devices.

Fig. 11 shows the panorama view of the test.

3. Test observations

As shown in Fig. 6, the strain gauge's numbers are used to represent the truss member's numbers here for the rest of the paper. For Case 1: with the wind speed of 15 m/s, in the process of applying equivalent wind load, there were no any significant deformation and displacement observed. After full loads applied on the scaled tower model, the support's displacement loading was applied step by step. When the support's displacement reached to 40 mm, the bottom cross bracing members F10, F11, B7, B8 and the horizontal diaphragm members F6, B4 were deformed significantly (see Figs. 12 and 13), then the test was ended. At that time, the out-of-plane displacements at the joint of the cross bracings F10-F11 and B7-B8 were 67 mm and 62mm, respectively. Significant buckling deformations were seen near the connecting bolt of the X-bracing members. The vertical downward deformations at the middle of the horizontal diaphragms members F6 and B4 were around 22 mm.

For Case 2: with the wind speed of 30 m/s, the bending deformations of the scaled tower's legs were observed when the equivalent wind load was applied. With the increase of support's displacement, the truss members of the scaled tower model were deformed significantly. When the support's displacement reached to 40 mm, the bottom cross bracing members F10, F11, B7, B8 and the horizontal diaphragm members F6, B4 were deformed significantly (see Figs. 14 and 15). The inward out-of-plane displacement at the joint of the cross bracing F10-F11 was about 35 mm and the outward out-of-plane displacement at the joint of the cross bracing B7-B8 was 32 mm. Very large deformations were formed in the lower parts of member F11 (105 mm) and B7 (113 mm). Due to the large deformations, significant warping deformations were formed in the members F11 and B7 at the joints to the tower's legs closed to the reaction wall. The horizontal diaphragm members F6 and B4 were deformed about 20 mm downward at the middle position. The tower's legs B and C

were bended significantly, with a maximum deflection of about 30 mm, especially at the lower joints to the cross bracings.

It can be found from the comparison between Case 1 and Case 2 that the out-of-plane displacements at the joints of the cross bracing F10-F11 and B7-B8 under wind of 30 m/s are both smaller than that under wind of 15 m/s. This is mainly because of the mutual restraint between the X-cross bracing members. Under the influence of supports' movements, the two members are all compressed and normally deformed out of the plane. Under the influence of the wind load, one member (F11, B7) is in compression while the other member (F10, B8) is in tension. The tensile member provides a support for the compressive member to reduce the out of plane displacement. Furthermore, the reduced displacement under the wind speed of 30 m/s is larger than that under the wind speed of 15 m/s because the former caused much larger tension force in member F11 (or B7) and provide stronger support for the other member (see Fig. 19 and Fig. 23). Therefore, influenced by the same supports' movement, the out-of-plane displacements corresponding to a wind speed of 30m/s are smaller than that under a wind speed of 15 m/s.

4. Test results and analysis

In this research two wind speeds of 15 m/s and 30 m/s were adopted to calculated applied wind loads. It was assumed that the value of wind load was proportional to the square of wind speed. Hence, the wind load with the wind speed of 30 m/s is about 4 time of the wind load with the wind speed of 15 m/s.

4.1 Case 1: Applied support's displacement with 15 m/s wind speed loading

Fig. 16 shows the displacements at the top corners of the scaled tower model against the applied wind load. In the figure, meters M1, M2 represent the horizontal displacements along the wind direction and meters M5 to M8 represent the vertical displacements. It can be seen that when the wind load was fully applied, the maximum horizontal displacement and vertical displacement at the top corners were 2.85 mm and 0.88 mm, respectively.

Fig.17 shows the horizontal displacements (measured by meters M1 to M4) at the top corners of the scaled tower model against applied support's displacement. It is clear that the horizontal displacements along the wind direction (measured by meters M1, M2) were increased almost linearly with the applied support's displacement. The maximum displacement was about 24.1 mm.

Fig. 18 shows the vertical displacements at the top corners of the scaled tower model against the applied support's displacement. It can be seen that all displacements were downward, with a maximum displacement of 2.06 mm. These were caused by the slightly bending of the tower's legs

subjected to the stretching of the supports.

In the process of applying support's displacement loading, the stresses in the structural members of the scaled tower model were changed mainly in the members within the planes F and B (see Fig. 6) which were along the direction of the applied support's displacement. The stresses within the structural members in the plane F are analysed as below.

In the rest of this paper, the tested stresses presented in the figures were calculated using the measured average strains at each measuring point multiplied by the steel elastic modulus. Fig. 19 shows the stresses of the cross bracing members in the plane F against the support's displacement. It can be seen that the first (F10 and F11) and third (F14) cross bracing members were subjected to compression, while the second cross bracing members (F12 and F13) were subjected to tension. When the support's displacement reached to 12.06 mm, the stresses of the bracing members were reached to their peak values. Then the stresses within the members were decreased with further displacement loading. This was due to the out-of-plane buckling of the bracing members.

4.2 Case 2: Applied support's displacement with 30 m/s wind speed loading

The displacements at the top corners of the scaled tower against the applied wind load are shown in Fig. 20. It can be seen that when the wind load was fully applied, the maximum horizontal displacement and vertical displacement at the top corners of the scaled tower were 15.31 mm and 3.59 mm, respectively.

The horizontal displacements (measured by meters M1 to M4) at the top corners of the scaled tower model against applied support's displacement are shown in Fig. 21. It is clear that the horizontal displacements along the wind direction (measured by meters M1, M2) were increased almost linearly with the applied support's displacement. The maximum displacement was about 35.15 mm.

Fig. 22 shows the vertical displacements at the top corners of the scaled tower model against the applied support's displacement. It can be seen that all displacements were downward, with a maximum displacement of 3.59 mm.

The stresses of the cross bracing members in the plane F against the support's displacement are shown in Fig. 23. It can be seen that the first (F10 and F11) and third (F14) cross bracing members were subjected to compression, while the second cross bracing members (F12 and F13) were subjected to tension. When the support's displacement reached to 10.59 mm, the stresses of the bracing members were reached to their peak values. The stresses within the members then were decreased with further displacement loading due to manly out-of-plane buckling of the first cross

bracing member F11.

4.3 Impact of wind load on the resistance of transmission towers against the ground deformation

In this paper all stresses presented are the mean axial stresses at the corresponding cross section of the members. The mean axial stresses are calculated from the strain values measured by the two strain gauges located at the flanges of each member (see Fig.10b). The FE simulation results reveal that the tower model firstly failed due to the stability failure of the cross bracing members. The mean axial stresses can help to identify the occurrence of stability failure of angle steel members which have large slenderness ratio. However, for those stability failed members, the mean axial stresses were always much smaller than the compressive strength of steel.

Fig. 24 shows the comparison of the axial stresses in the member F10 against the support's displacement under the wind speed loading conditions of 0 m/s [28], 15 m/s and 30 m/s. At 0 m/s wind speed loading condition, the scaled tower model was only subjected to vertical self-weight loading, hence, the member F10 was under compression. When the wind speed increased to 15 m/s, the member F10 was subjected to tension before the support's displacement was applied. The initial tensile stress in the member was 4.90 MPa. When the wind speed increased to 30 m/s, the tensile stress in the member F10 was reached to 12.92 MPa.

When the horizontal stretching support's displacement was applied to the scaled tower model, the compressive stress was developed within the member F10 and increased to a peak value then decreased afterward. It can be seen from the figure that the wind load induced tensile stress which partially balanced the compressive stress caused by the support's displacement. Therefore, the peak compressive stresses in F10 were decreased with increasing of wind speed, which were 62.13 MPa, 51.31 MPa and 24.38 MPa, respectively, under the 0, 15 m/s and 30 m/s wind speeds. The applied support's displacements corresponding to the peak stresses were 13.06 mm, 12.06 mm and 11.35 mm, respectively.

Fig. 25 shows the axial stresses in the diagonal member F11 versus the support's displacement under three wind speed loading conditions. It can be seen that F11 was in compression under initial wind load, before the support's displacement was applied. The compressive stress in F11 increased linearly with increasing support's displacement. When the support's displacement reached to a limit value, the compressive stress started to decrease with increased support's displacement. When the support displacement reached to 40 mm, the compressive stresses within the member F11 were still greater than 20 MPa for all three wind speed loading conditions. This indicated that the tower structure as a whole still has the capability to resist the ground deformation even if some truss

members were failed due to buckling deformations. The main reason for this is that the tower structure is the high order indeterminate structure assembled with multi angle steel trusses.

It also can be seen from Fig. 25 that the compressive stress in F11 was increased with wind speed. Compared with the case of zero wind speed, the compressive stresses were increased by 1.00% and 7.87% corresponding to wind speeds of 15 m/s and 30 m/s. From the test observation it is clear that the failure of the scaled tower model was mainly caused by the compressive failure of the truss members. The member F11 was the first member to fail by compression. The applied support's displacement related to the maximum compressive stress within the truss member is the *limit support's displacement* which the scaled tower model can sustain. As shown in Figs. 24 and 25, the limit support displacement was decreased with wind speed increased. Compared with the case of zero wind speed, the limit support's displacements were decreased by 7.7% and 18.9% at wind speeds of 15 m/s and 30 m/s. These results indicated that the wind load can introduce adverse influence on the resistance of the transmission tower to the ground surface deformation. Therefore, for assessing the safety of transmission towers under the ground surface deformation, it is necessary to consider the impact of wind load.

5. Validation of the developed FE model

As mentioned in the introduction section, one of the main objectives of this research is to develop a FE model using ANSYS for modelling the 110 kV single-circuit power transmission tower and validate the FE model by the test data generated in this research. The FE model is based on the previous developments [28] in which the tower is under wind load only. This FE model has been extended here to consider the combined effects for both horizontal ground moving and wind load. Hence, the focus of this section is on the validation of extended FE model subjected to horizontal ground movement under wind load conditions.

As mentioned in the previous sections, a FE model by using ANSYS was developed to model the behaviour of the scaled tower model and the original whole tower under ground surface deformation. Hence, in this section the scale tower models were modelled and compared with the test results. Two wind speed loading conditions (15 m/s and 30 m/s) were used here to validate the FE model developed. Then the validated model will be used in the future to assess the behaviour of the 110 kV single-circuit power transmission tower subjected to ground surface deformations under wind loading conditions and to improve the safety design of the power transmission tower under real working conditions.

Fig. 26 shows the failure patterns of the scaled tower model which were obtained from the test and FE modelling. In the figure, the failure of the tower is marked by the out-of-plane stability failure of the cross bracing member F11. It is evident that the failure pattern predicted by the FE model is similar to the test.

Fig. 27 shows the comparison of predicted and measured horizontal displacements at the position of M2 (see Fig. 8) on the top of the scaled tower model versus applied support's displacement for different wind speed loading conditions. It is clear that predicted and measured values were in good agreement.

In the FE modelling the predicted stresses for each member were calculated using the predicted member's axial force divided by the cross-section area of the member. Figs. 28 and 29 show the comparisons of predicted and measured stresses within the truss members F11 and F14 against the applied support's displacement for the two wind speed loading conditions. The member F11 was the bottom diagonal member of the scaled tower model and was the first one to fail. The member F14 was the top cross bracing member (see Fig. 6). Hence, F11 and F14 were the representative structural members of the scaled tower model. It is evident that the predicted and measured ultimate support's displacements, in which stresses started to decrease, were agreed well for all cases. Reasonable agreement between predicted and measured stresses was achieved for all cases as well. Therefore, FE model developed in this research has the capability to model transmission towers subjected to the ground movement under wind load conditions with a reasonable accuracy. Hence, the FE procedure can be adopted for further study in the future to fully understand the failure mechanisms of power transmission towers subject to coupled wind load and the ground deformation.

6. Conclusions

In this research, two 1:2 scaled tower models for a typical 110 kV transmission tower were designed and fabricated. The scaled tower models were tested subjected to the horizontal ground surface stretching movements under two wind load conditions. The deformations of the scaled tower models and stresses within the different bracing members were full measured. The developed FE

model was validated using the test data. The main conclusions are drawn as follows:

- The designed 1:2 scaled tower models can reasonably represent the behaviour of whole tower subjected to the horizontal support's movement under different wind loading conditions.
- The key failure pattern of the scaled towers model was the out-of-plane buckling of the first cross bracing members F10, F11, B7 and B8. With increased wind load, the bottom cross bracing members were failed at less support's displacement.
- The peak stress in bracing member F11 was increased considerably with the increased wind speed and the corresponding ultimate support's displacement at the peak stress was decreased. Compared with the case of zero wind speed, the maximum stress in the member F11 was increased by 7.87% and the limit support displacement was decreased by 18.9% for the wind speed of 30 m/s. Hence，the wind load has significant adverse effect on the resistance of the power transmission towers to the ground surface deformation.
- The FE model developed in this research can be used to study the structural behaviour of power transmission towers subjected to the ground surface deformation under different wind loading conditions.

Acknowledgements

This research was supported by the China State Grid Corporation under the grant No. 0711-14OTL24311163. The authors gratefully appreciate this support.

References

[1] Battista R.C., Rodrigues R.S., Pfeil M.S., Dynamic behaviour and stability of transmission line towers under wind forces. Journal of Wind Engineering and Industrial Aerodynamics, 2003, 91: 1051–1067.

[2] Kudzys A., Safety of power transmission line structures under wind and ice storms. Engineering Structures, 2006, 28: 682–689.

[3] Savory E., Parke G.A.R., Disney P., Toy N., Wind-induced transmission tower foundation loads: A field study-design code comparison. Journal of Wind Engineering and Industrial Aerodynamics, 2008, 96: 1103–1110.

[4] Albermani F., Kitipornchai S., Chan R.W.K., Failure analysis of transmission towers. Engineering Failure Analysis, 2009, 16: 1922–1928.

[5] Hamada A., El Damatty A.A., Behaviour of guyed transmission line structures under tornado wind loading, Computers and Structures, 2011, 89: 986–1003.

[6] Kyung D., Choi Y., Jeong S., Lee J., Improved performance of electrical transmission tower structure using connected foundation in soft ground. *Energies,* 2015, *8*: 4963-4982.

[7] Brown R.J.E., Permafrost in Canada-its influence on northern development. Toronto and Buffalo, USA: University of Toronto Press, 1973.

[8] Yang F., Yang J., Han J., Study on the limited values of foundation deformation for a typical UHV transmission tower. IEEE Transactions on Power Delivery, 2010, 25(4): 2752-2758.

[9] Zhenhua S., Settlement and the treatment plan for the foundation of the tangent towers of the transmission lines in the goaf of coal mine. Shanxi Power Technology, 1997, 17: 18-20.

[10] Jia L., Zai H, Design and operation of power line in mining area. Beijing: China Electric Power Press, 2015.

[11] Zhang Y., Present situation and countermeasures of disaster prevention for transmission lines. Power of East China, 2006, 34(3): 28-31.

[12] Moon B.W., Park J.H., Lee S.K., Kim J., Kim T., Min K.W., Performance evaluation of a transmission tower by substructure test. Journal of Constructional Steel Research, 2009, 65: 1-11.

[13] Xie Q., Sun L., Lin H., Chen Q., Experimental study on wind-resistant ultimate load-carrying capacity of 500 kV transmission tower. High Voltage Engineering, 2012, 38(3): 712-719.

[14] Momomura Y, Marukawa H, Okamura T, Hongo E., Ohkuma T., Full-scale measurements of wind-induced vibration of a transmission line system in a mountainous area. Journal of Wind Engineering and Industrial Aerodynamics, 1997, 72: 241-252.

[15] Okamura T., Ohkuma T., Hongo E., Okada H., Wind response analysis of a transmission tower in a mountainous area. Journal of Wind Engineering and Industrial Aerodynamics, 2003, 91: 241-252.

[16] Yasui H., Marukawa H., Momomura Y., Ohkuma T., Analytical study on wind-induced vibration of power transmission towers. Journal of Wind Engineering and Industrial Aerodynamics, 1999, 83(2): 431-441.

[17] Mara T.G., Hong H.P., Effect of wind direction on the response and capacity surface of a transmission tower, Engineering Structure, 2013, 57:493-501.

[18] Mara, T.G.; Hong, H.P.; Lee, C.S.; Ho, T.C.E., Capacity of a transmission tower under downburst wind loading, Wind and Structure, 2016, 22(1):65-87.

[19] Stump D.E. Jr., Grouting to control coal mine subsidence. Geotechnical Special Publication, 1998, Grouts and Grouting (S1): 128-138.

[20] Bruhn R. W., Ferrell, J.R., Luxbacher, G.W., The structural response of a steel-lattice transmission tower to mining related ground movements. Proceedings of the 10th International Conference on Ground Control in Mining, West Virginia University, Morgantown, WV, 1991, 301-306.

[21] White B. H., Outcomes of the independent inquiry into impacts of underground coal mining on natural features in the Southern Coalfield-An Overview. Proceedings of the 2009 coal operators conference, University of Uollongong, NSW, Australia, 2009, 112-123.

[22] Yuan G.L., Yang G.Y., Zhang Y.F., Regularities on internal force and structure deformation of transmission tower influenced by ground deformation. Journal of China Coal Society, 2009, 34(8): 1043-1047.

[23] Yuan G.L., Zhang Y.F., Li S., Liu T., Ji Y., Model experiment on anti-deformation performance of self-supporting transmission tower in subsidence area. International Journal of Mining Science and Technology, 2012, 22(1): 57-62.

[24] Shu Q.J., Yuan G.L., Guo G.L., Zhang Y.F., Research on the composite foundation anti-deformation performance and optimal thickness of electricity transmission towers in mining subsidence area. Journal of Disaster Prevention and Mitigation Engineering, 2012, 32(3), 294-298.

[25] Li B., Jian M., Zhang D., Finite element analysis of foundation settlement of 220kv transmission tower with independent foundation. Applied Mechanics and Materials, 201-202, 2012, 602-607.

[26] Manis P., Bloodworth A.G., Climate change and extreme wind effects on transmission towers. Proceedings of the Institution of Civil Engineers, Structures and Buildings, 2017, 170(2), 81-97.

[27] Shu, Q., Yuan, G., Huang, Z., and Ye, S., The behaviour of the power transmission tower subjected to horizontal support's movements", Engineering Structures, 2016, 123, 166–180.

[28] Ye S., Study on ground deformation and wind resistant performance of 110 kV transmission tower in mining subsidence area. MSc Dissertation, China University of Mining and Technology, 2015.

List of Tables and Figures

List of Tables

Table 1 The sectional properties of the members for prototype tower substructure and scaled tower model.

Member Type	Prototype tower substructure			Scaled tower model		
	Dimension（mm×mm）	Steel grade	Section area（mm^2）	Dimension（mm×mm）	Steel grade	Section area（mm^2）
Tower leg	L90×7	Q345	1230	L40×4(hot-rolled)	Q235	309
Horizontal Diaphragm	L56×4	Q235	439	L28×2(cold-worked)	Q235	112
Diagonal Member	L50×4	Q235	390	L25×2(cold-worked)	Q235	100
	L45×4	Q235	349	L23×2(cold-worked)	Q235	92
	L40×3	Q235	236	L20×1.5(cold-worked)	Q235	60
Auxiliary Truss member	L40×3	Q235	236	L20×1.5(cold-worked)	Q235	60

Table 2 Measured yield strengths of angle steel for the scaled tower model (MPa).

Leg (Hot-rolled Angle L40×4)	Diagonal Member (Cold-Worked Angle, Flange Thick 2mm)	Auxiliary Member (Cold-Worked Angle, Flange Thick 1.5mm)
323.3	309.2	313.1

Table 3 Wind loads and vertical loads acting on the prototype of whole tower (N).

Load Category		Wind Speed (m/s)		
		0 m/s	15 m/s	30 m/s
Horizontal Wind Load	Conductor	0	1638	4915
	Insulator and Accessories	0	112	337
	Ground Wire	0	1033	3098
Vertical Load	Conductor	6964	6964	6964
	Insulator and Accessories	1182	1182	1182
	Ground Wire	5977	5977	5977
	Self-weight of Tower	27979		

List of Figures

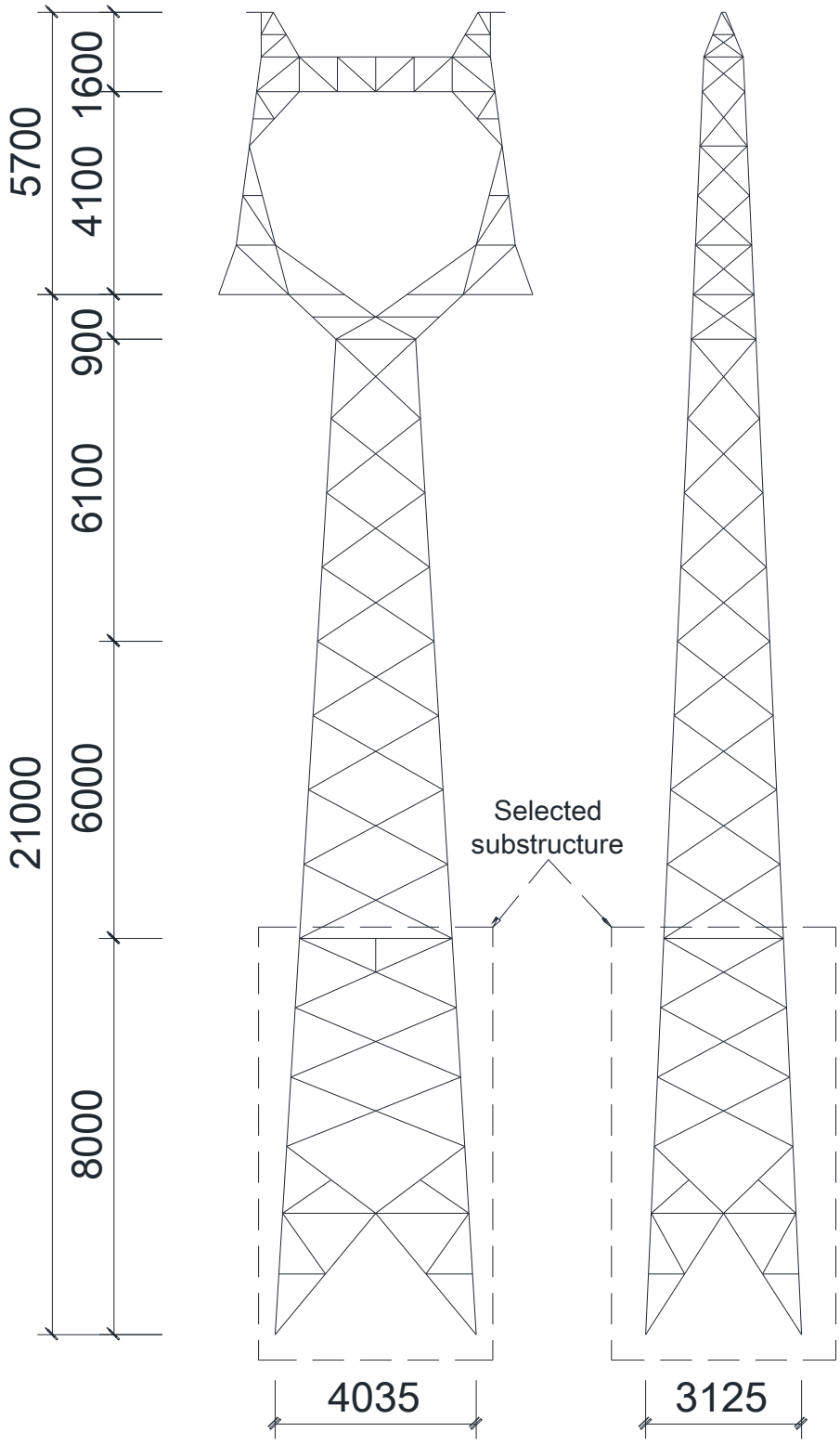

Fig. 1 A prototype of 110 kV single circuit transmission tower (all dimensions in mm).

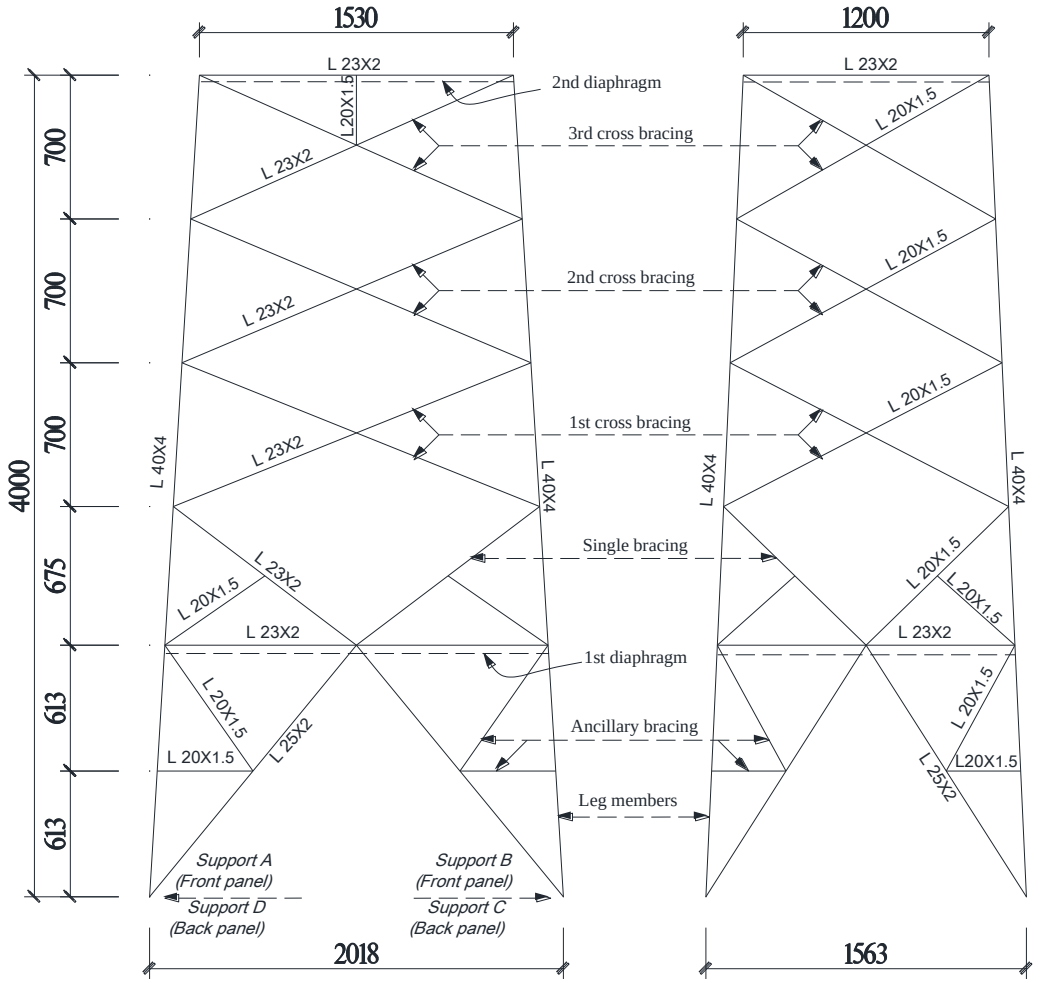

Fig. 2 The 1:2 scaled tower model (all dimensions in mm).

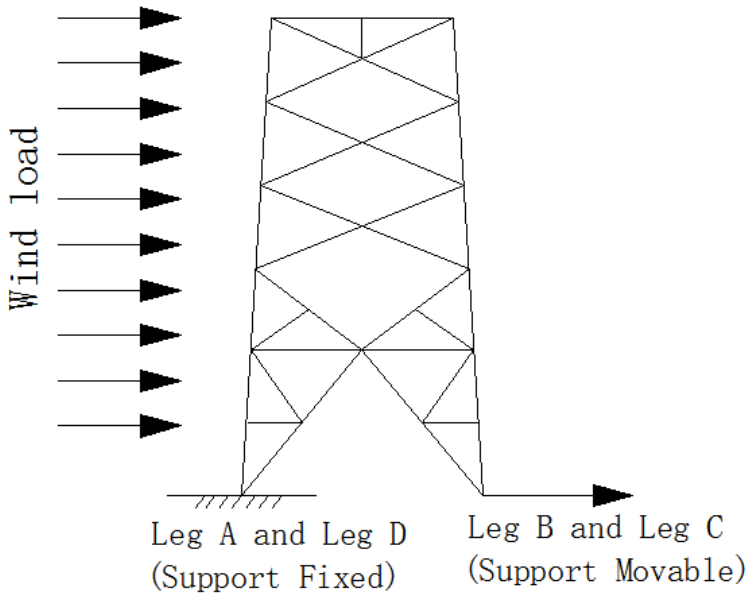

Fig. 3 The directions of wind load and displacement load.

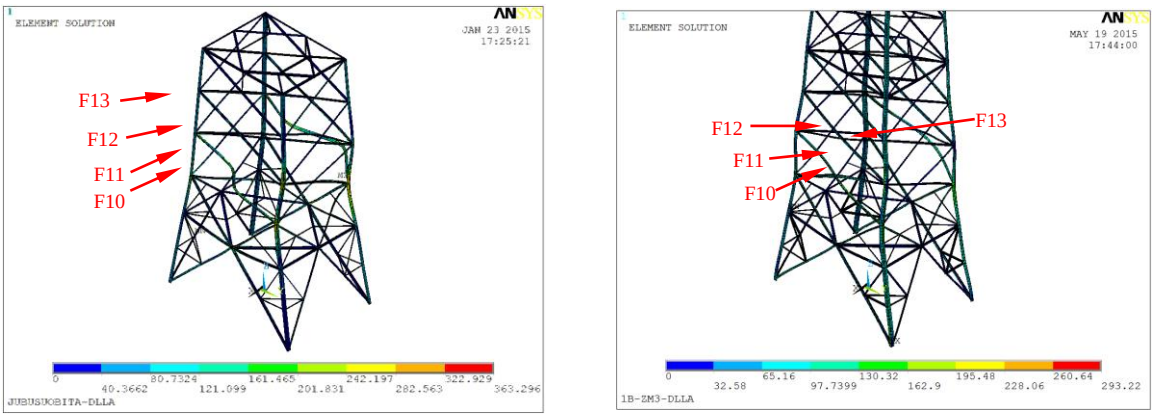

(a) The scaled tower model

(b) The original whole tower

Fig. 4 The comparison of predicted deformed shapes between the scaled tower model and original whole tower (enlarged 20 times).

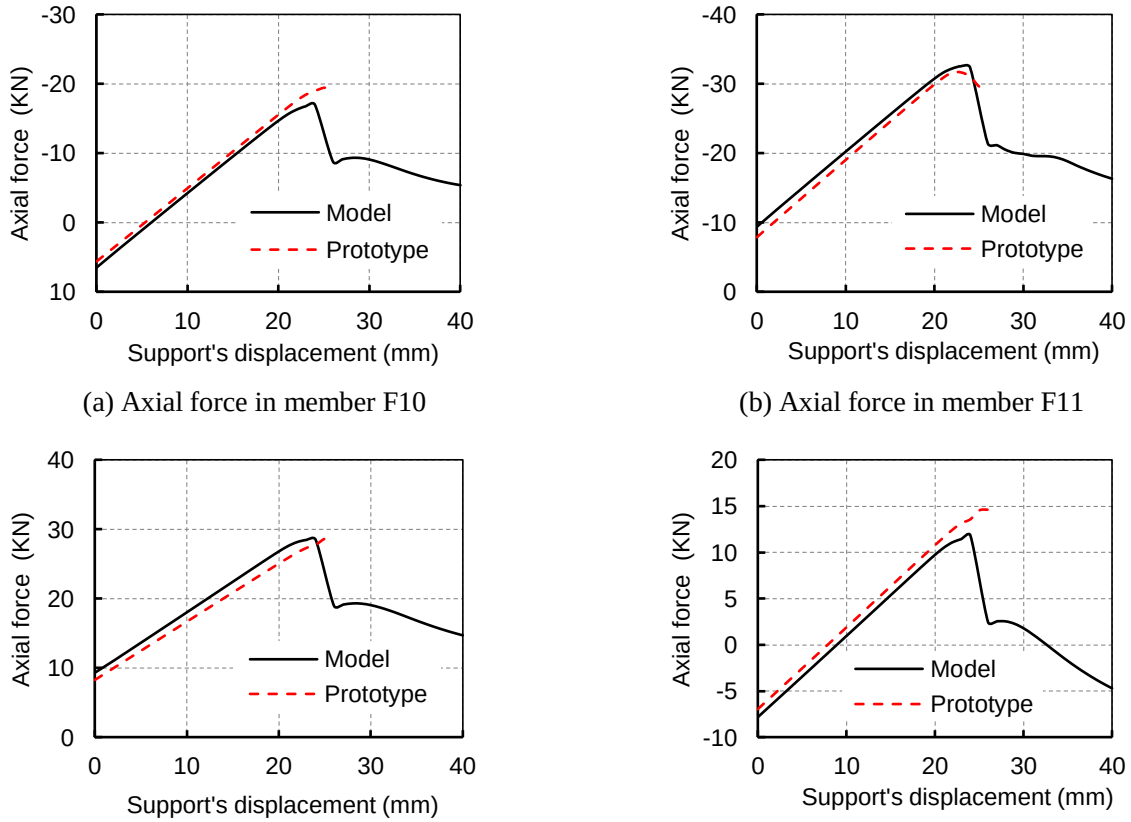

(a) Axial force in member F10

(b) Axial force in member F11

(c) Axial force in member F12

(d) Axial force in member F13

Fig. 5 The comparisons of the axial forces of some key members for both FE analyses.

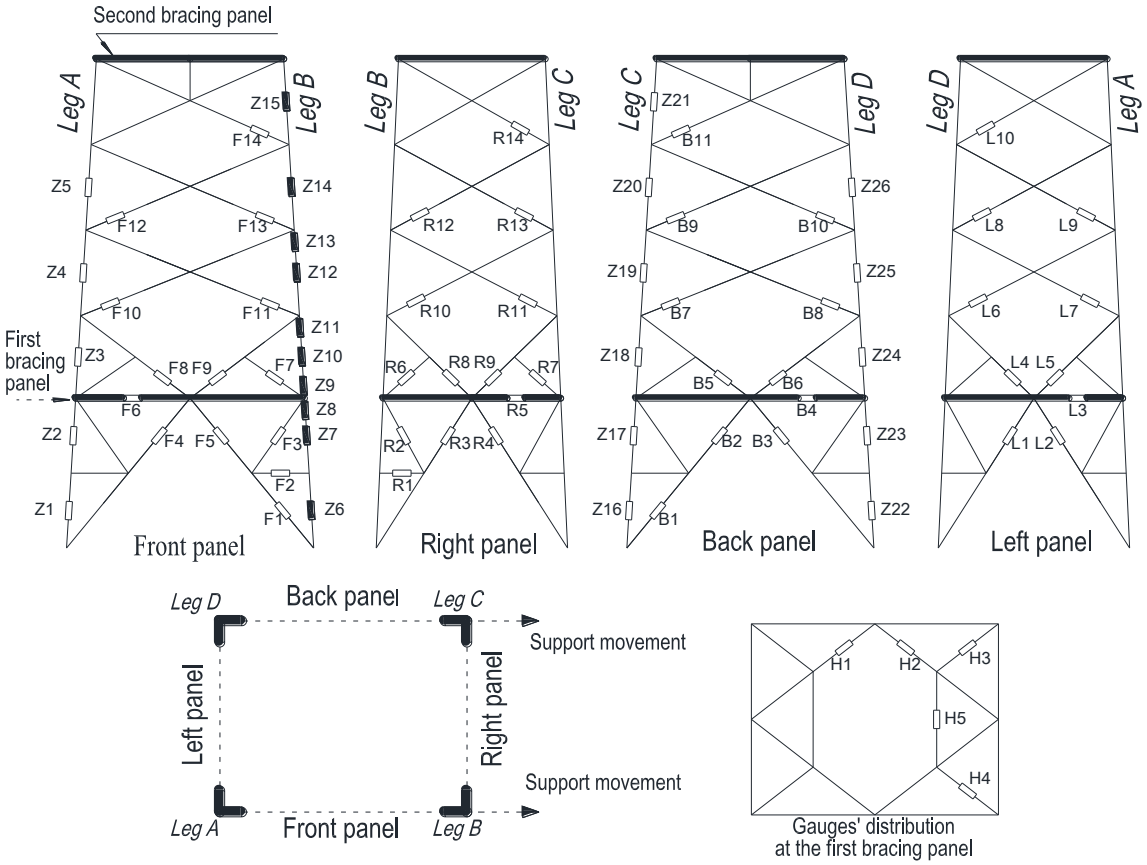

Fig. 6 The arrangement of the strain gauges in the truss members of the scaled tower model.

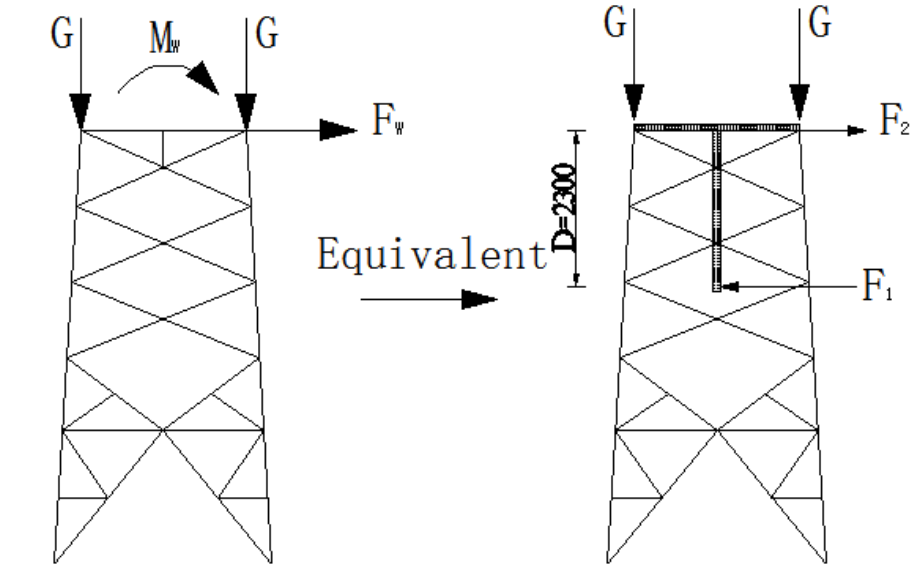

(a) Actual loads (b) Equivalent loads

Fig. 7 Applied equivalent loads on the scaled tower model.

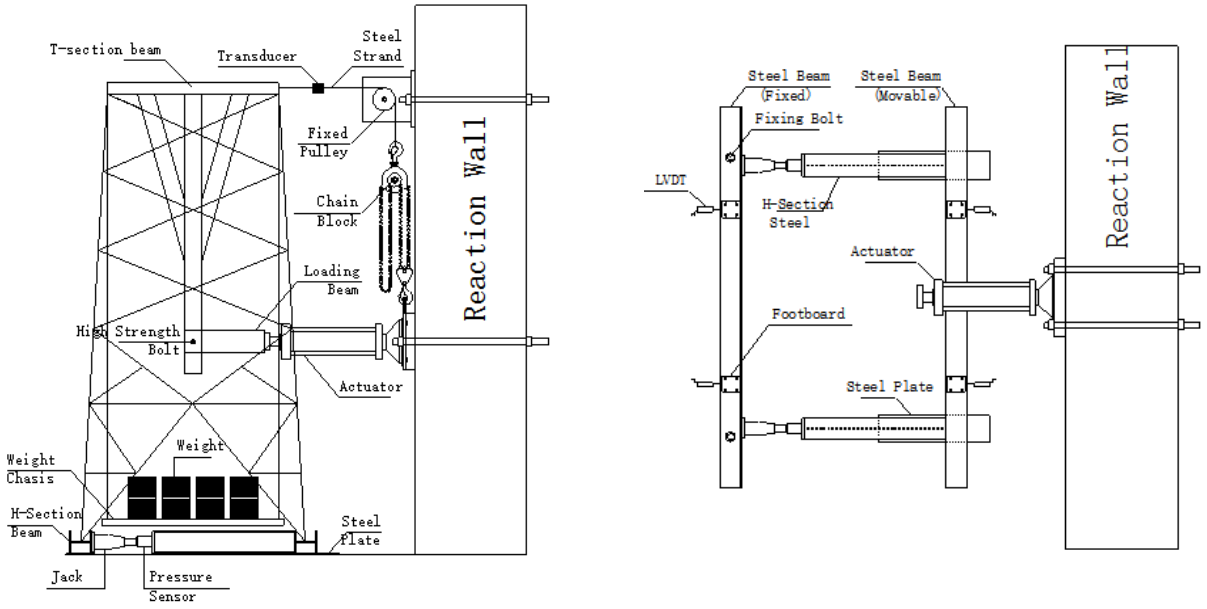

(a) Side Elevation (b) Plan View

Fig. 8 Loading scheme for the scaled tower model.

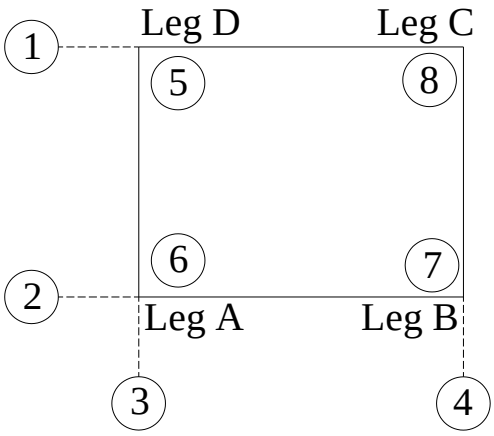

Fig. 9 Arrangement of 8 guyed displacement meters at 4 top corners of the scaled tower model.

(a) Strain gauges at positions Z6-Z15 on the tower's leg B

(b) Strain gauges fixed on other truss members

Fig. 10 Details of strain gauges attached on the structural members.

Fig. 11 Panorama view of the test.

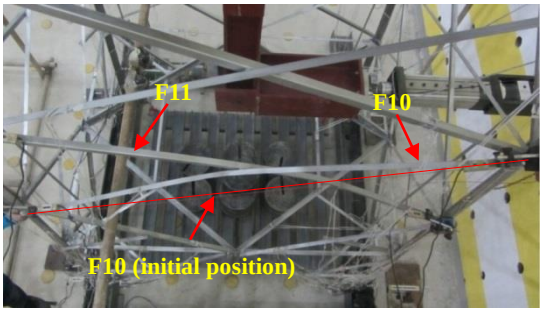

(a) Deformations of the members F10 and F11

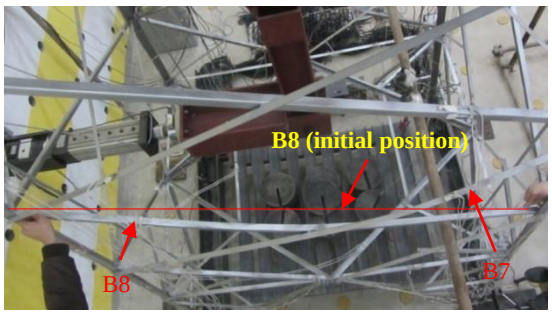

(b) Deformations of the members B7 and B8

Fig. 12 Deformation of the first cross bracing members for Case 1.

Fig. 13 Deformation of horizontal diaphragm for Case 1.

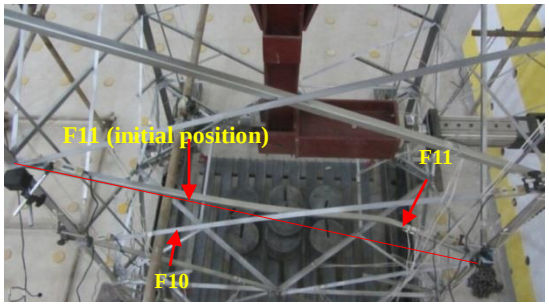

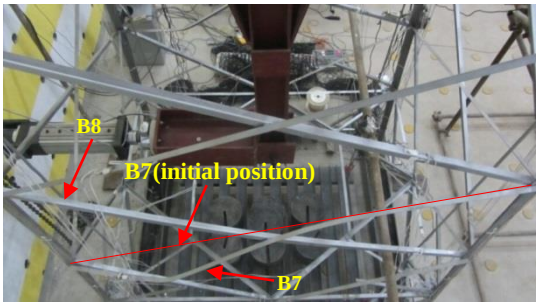

(a) Deformations of the members F10 and F11 (b) Deformations of the members B7 and B8

Fig. 14 Deformation of the first cross bracing members for Case 2.

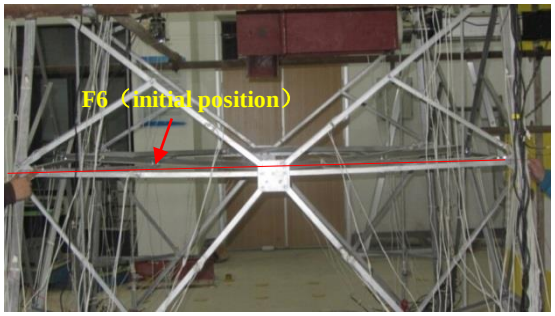

Fig. 15 Deformation of horizontal diaphragm for Case 2.

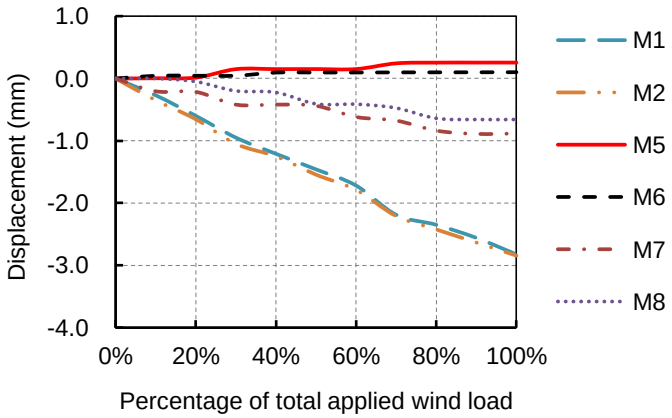

Fig. 16 The displacements at the top corners of the scaled tower model against the wind load (Case 1).

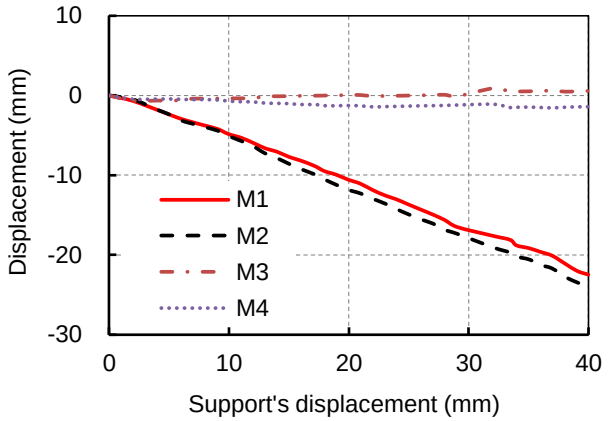

Fig. 17 The horizontal displacements at the top corners of the scaled tower model against the support's displacement (Case 1).

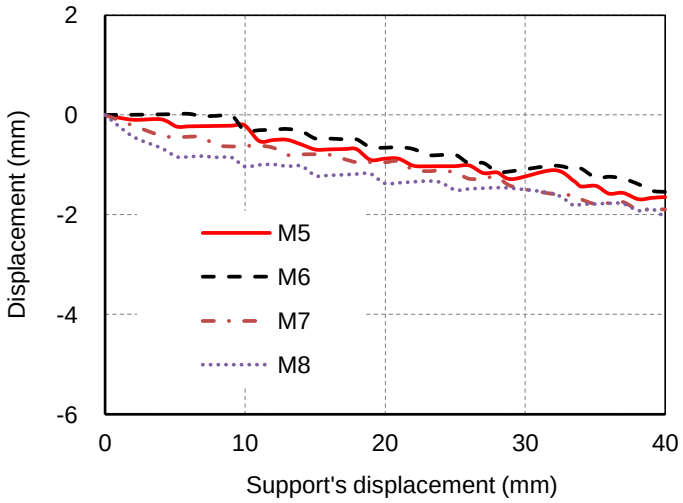

Fig. 18 The vertical displacements at the top of the scaled tower model against support's displacement (Case 1).

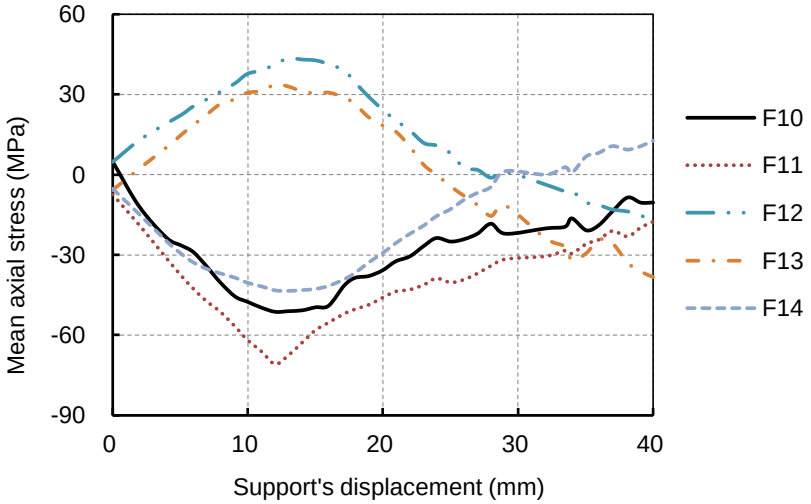

Fig. 19 The developments of mean axial stress within in the cross bracing members (Case 1).

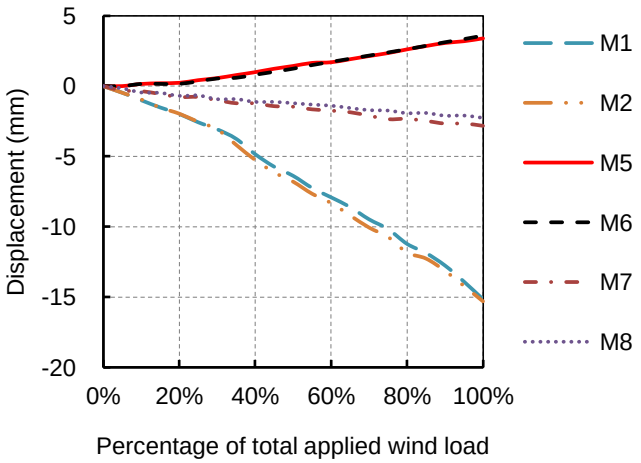

Fig. 20 The displacements at the top corners of the scaled tower model against the wind load (Case 2).

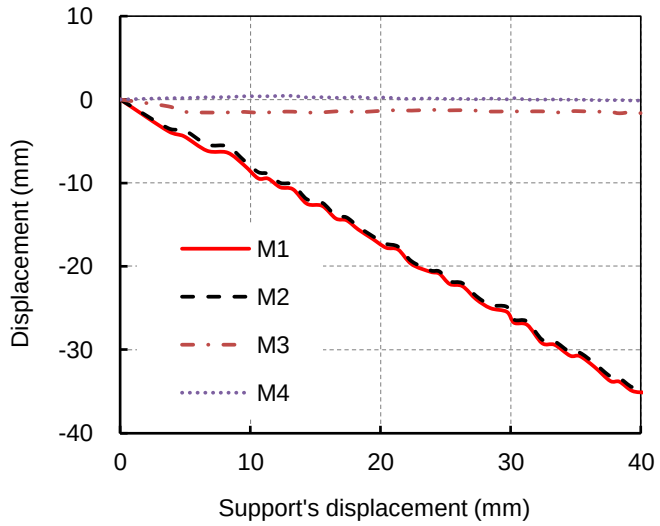

Fig. 21 The horizontal displacements at the top corners of the scaled tower model against the support's displacement (Case 2).

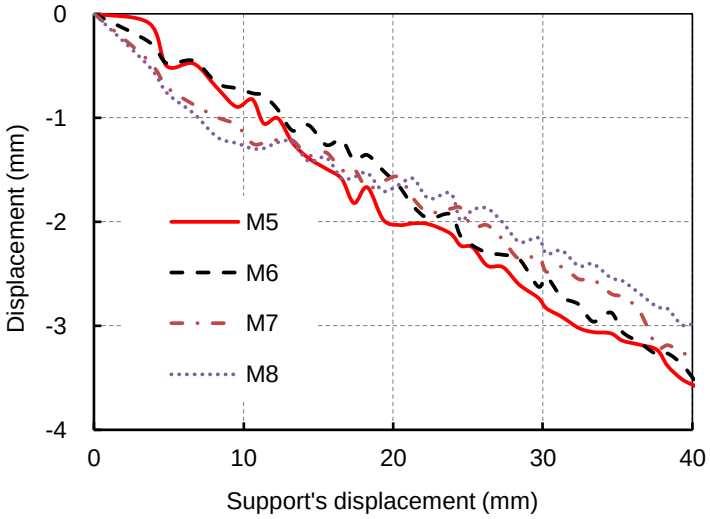

Fig. 22 The vertical displacements at the top of the scaled tower model against support's displacement (Case 2).

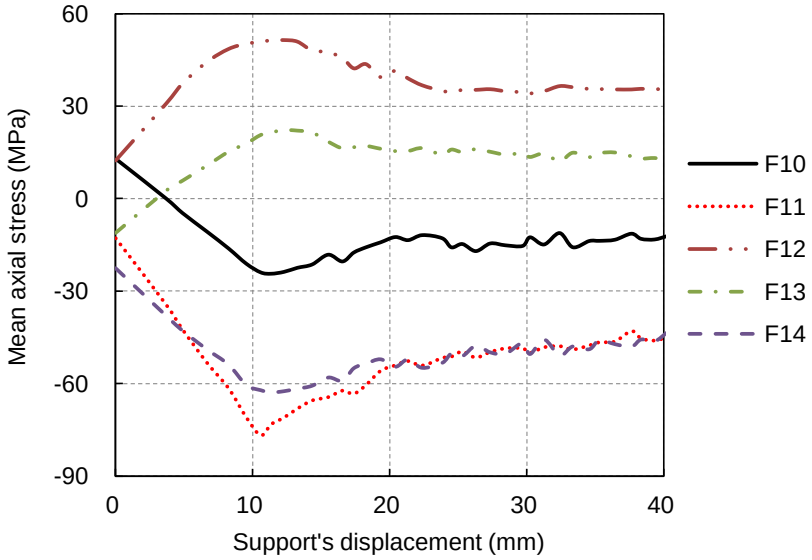

Fig. 23 The developments of mean axial stress within the cross bracing members (Case 2).

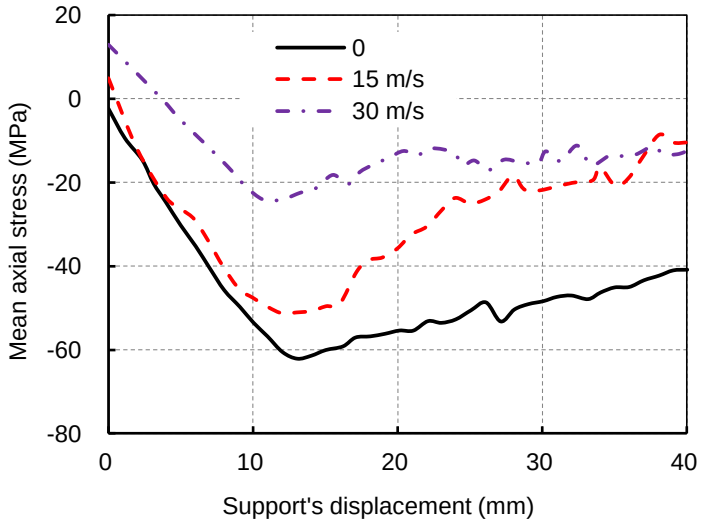

Fig. 24 Comparison of mean axial stresses in member F10 under different wind speed loading conditions.

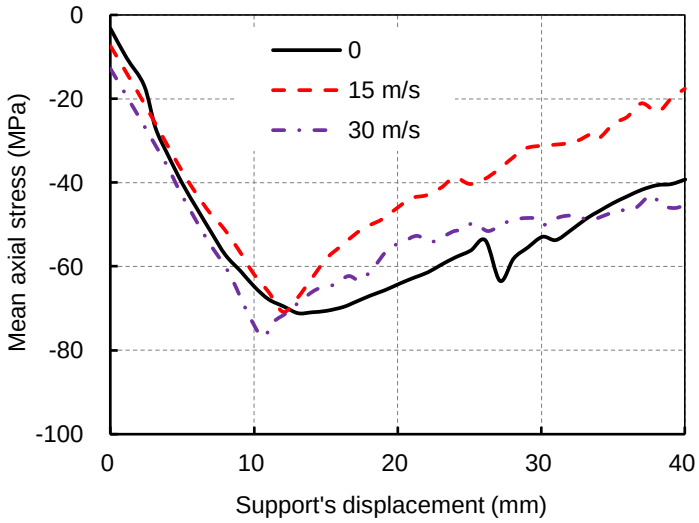

Fig. 25 Comparison of mean axial stresses in member F11 under different wind speed loading conditions.

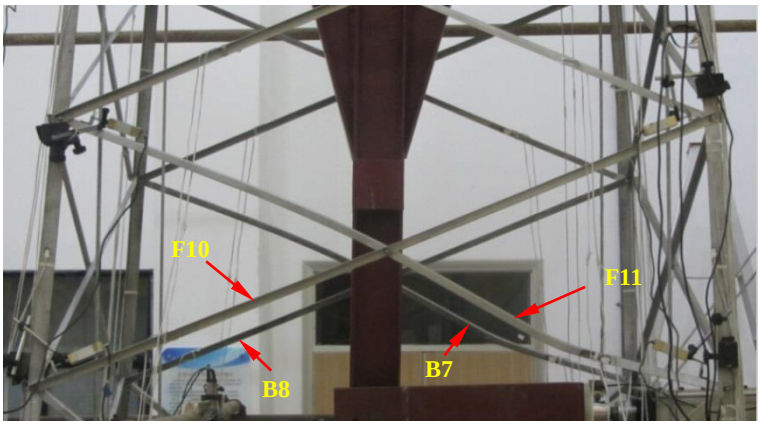

(a) Test failure pattern of the scaled tower model

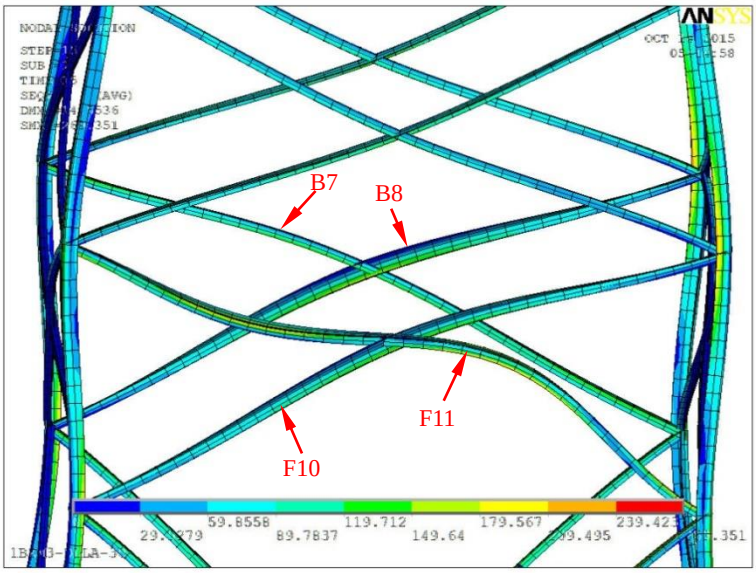

(b) Predicted failure pattern of the scaled tower model

Fig. 26 Comparison of predicted and tested failure patterns of the first cross bracing at wind speed of 30 m/s.

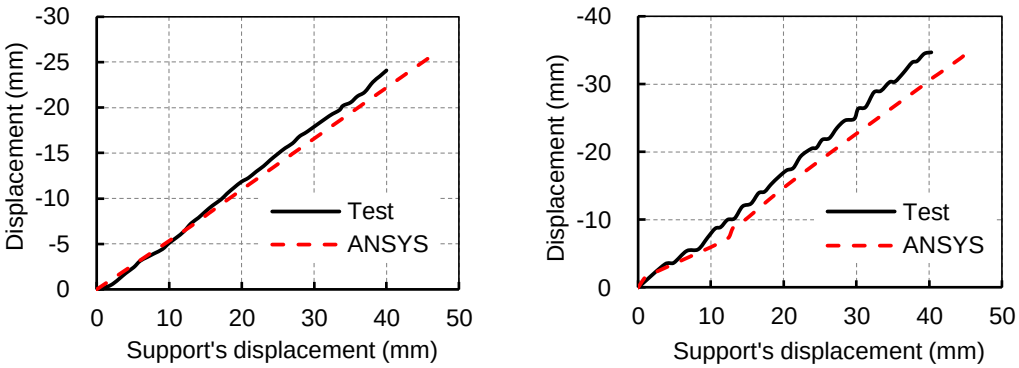

(a) Wind speed of 15 m/s (b) Wind speed of 30 m/s

Fig. 27 Comparison of predicted and measured horizontal displacements at the position of M2 on the top of the scaled tower model for two wind speed loading conditions.

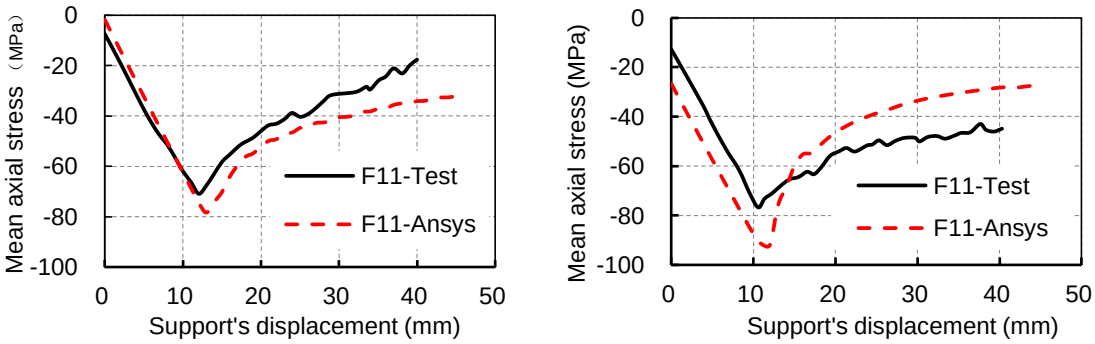

(a) 15m/s (b) 30m/s

Fig. 28 Comparison of predicted and measured mean axial stresses in member F11 vs support's displacement for two wind speed loading conditions.

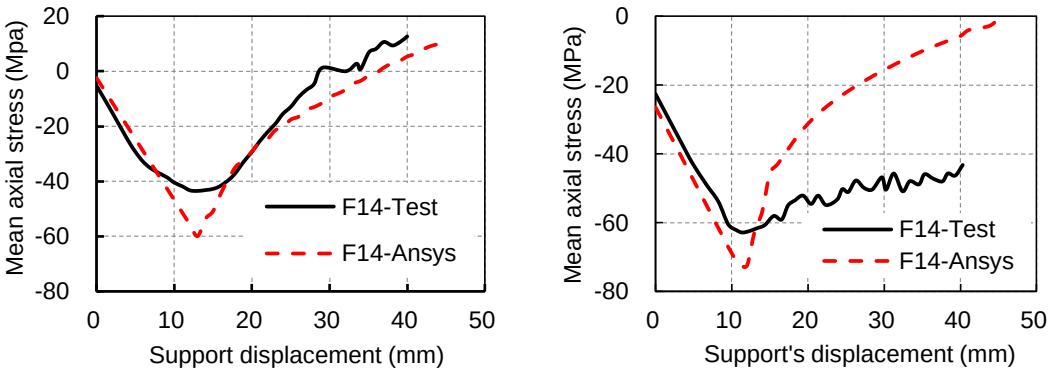

(a) 15m/s (b) 30m/s

Fig. 29 Comparison of predicted and measured mean axial stresses in member F14 vs support's displacement for two wind speed loading conditions.